

# PROCEEDINGS OF SPIE

[SPIDigitalLibrary.org/conference-proceedings-of-spie](https://spiedigitallibrary.org/conference-proceedings-of-spie)

## Is ZnO as a universal semiconductor material an oxymoron?

B. Hussain, B. Kucukgok, M. Y. A. Raja, Benjamin Klein,  
N. Lu, et al.

**SPIE.**

## Is ZnO as a universal semiconductor material an oxymoron?

B. Hussain<sup>\*a</sup>, B. Kucukgok<sup>a</sup>, M. Y. A. Raja<sup>a,b</sup>, B. Klein<sup>c</sup>, N. Lu<sup>a,d</sup>, and I. T. Ferguson<sup>a</sup>

<sup>a</sup>Dept. of Electrical and Computer Engineering, University of North Carolina at Charlotte, 9201 University City Blvd, Charlotte, NC 28223, USA; <sup>b</sup>Dept. of Physics and Optical Science, University of North Carolina at Charlotte, 9201 University City Blvd, Charlotte, NC 28223, USA; <sup>c</sup>Dept. of Electrical and Computer Engineering, Georgia Institute of Technology, North Ave NW, Atlanta, GA 30332, USA; <sup>d</sup>Dept. of Engineering Technology, University of North Carolina at Charlotte, 9201 University City Blvd, Charlotte, NC 28223, USA

### ABSTRACT

The wide-bandgap semiconductor ZnO has gained major interest in research community for its unique properties and wide range of applications. In this review article, we present synthesis techniques and a few emerging applications for ZnO. Common techniques for growing ZnO films are discussed briefly, and a detailed discussion of MOCVD growth of ZnO is provided citing previous experimental reports on this technique by our group and others. A few important and distinctive uses of ZnO are discussed for various applications focusing on the current limitations of ZnO to realize its feasibility in these applications.

**Keywords:** Zinc oxide, MOCVD, TFTs, HEMTs, LEDs, neutron detection, thermoelectricity

### 1. INTRODUCTION

With the increased demand for high power and high temperature optoelectronic devices, wide-bandgap semiconductor materials have drawn major attention from researchers and industry in recent years. These materials have additional advantages including light emission/absorption in the UV/visible range, broad transmission, a large piezoelectric effect, high breakdown voltages, and low electronic noise. Zinc oxide (ZnO) is a compound semiconductor with wide bandgap tunable from 3 to 4 eV with doping or alloying. Its unique advantages over other II-VI and III-V wide-bandgap materials include lower processing costs, low-level of toxicity, and natural abundance. The relatively small refractive index of ZnO compared to GaN results in larger exciton binding energy (60 meV), much greater than  $kT$  at room temperature guarantees efficient luminescent and photovoltaic characteristics. The wurtzite structure with tetrahedral arrangement is the most stable form of ZnO with lattice parameters  $a=3.25 \text{ \AA}$  and  $c=5.21 \text{ \AA}$  which make it a potential substrate for another widely used material, gallium nitride (GaN) [1-4]. This allows fabrication of useful heterostructures for complex optical and electronic devices. The  $c/a$  ratio of ZnO wurtzite structure is 1.603 which is very close to the ideal ratio (1.633) for highly stable structures. The non-centrosymmetric wurtzite structure of ZnO gives rise to large piezoelectric and pyroelectric coefficients resulting in its potential use in mechanical sensors and nanogenerators [5]. Extensive research has been carried out on the fabrication and use of ZnO nanostructures owing to its stable morphological structure. In addition, the use of amorphous oxide semiconductors has appeared as a new technology which may overcome many of the problems associated with conventional silicon technology [6]. A review of recent advances in oxide semiconductors shows that amorphous ZnO appears having most desirable properties of all the amorphous oxide semiconductors [7]. The high electron mobility and wide bandgap of ZnO make it a suitable candidate for fabrication of high electron mobility transistors (HEMTs) [8-10]. Aluminum- or gallium-doped ZnO has recently gained much attention as a suitable replacement for indium tin oxide (ITO), which is comparatively expensive material and less stable in hydrogen plasma, in fabrication of transparent conducting oxide (TCO) thin films [11-16].

Previously, our group reported several investigations of ZnO as a potential substrate technology for GaN based devices due to its close lattice match, stacking order match, and similar thermal expansion coefficient [17-20]. In later stages of this work, a sapphire transition layer was deposited on ZnO using atomic layer deposition (ALD) to prevent zinc and oxygen diffusion into the GaN epilayers as well as to assist nitride epilayer growth for improved film quality [21-25]. It has been demonstrated that the lattice match of ZnO substrates can be exploited for the suppression of phase separation in InGaN and AlGaIn layers. Using a custom-built metal organic chemical vapor deposition (MOCVD) system, we have studied reactor dynamics of ZnO growth by exploring the influence of different parameters and growth conditions on the structural, optical, and electrical quality of ZnO films. In addition, some novel characteristics of ZnO such as magnetic

properties for spintronic applications [26-29], reflective second harmonic generation [30], optical waveguiding [31], and neutron detection [32] have been investigated. Recently, we have grown ZnO thin films with different thicknesses on sapphire substrates using MOCVD to demonstrate that crystal quality degrades with increasing film thickness due to the lattice mismatch with the substrate and growth rate significantly decreases with increasing chamber pressure [33].

In this paper, we present a brief review of synthesis and applications of ZnO thin films and nanostructures with special emphasis on the metal oxide chemical vapor deposition (MOCVD) technique. The next section explains synthesis techniques commonly used to grow zinc oxide layers. The following section describes important applications of ZnO currently under investigation such as thin film transistors (TFTs) and HEMTs, UV emitters and detectors, and neutron detection. Details of these applications are given and important experimental results presented by our group as well as other relevant reports are reviewed and discussed.

## 2. SYNTHESIS TECHNIQUES AND CHARACTERIZATION

Various established methods of semiconductor crystal growth have been used by different groups to grow high quality ZnO on a wide range of substrates. Molecular beam epitaxy (MBE) is one of the best technologies to obtain ZnO thin films with high crystallinity and purity. Heterostructure devices were prepared by growing a single layer of MgZnO on Zn-polar ZnO single crystal substrates for HEMT applications [8]. Another group contemporaneously achieved fabrication of MgZnO/ZnO heterostructures on c-plane sapphire substrates by radical source MBE [9]. Recently, our group has experimentally investigated bulk ZnO grown by MBE to confirm theoretical predictions of the true origin of intrinsic n-type conductivity in ZnO [34]. The proven repeatability of experimental results proves the reliability of the MBE method. The main disadvantages of MBE are the high cost to employ and maintain the system, the low growth rate, and the graded edges of the as-grown film.

Evaporation of ZnO is particularly difficult because of its high melting point. Therefore, magnetron sputtering or plasma vapor deposition (PVD) is an alternate method to grow ZnO films [35, 36]. In this process, a positively charged source plasma is generated and accelerated towards negatively charged electrode (target). The contamination problem caused by diffusive transport is a shortcoming of magnetron sputtering. Furthermore, the sputtering method lacks reproducibility due to little control over the film structure [10]. Multiple layer growth is challenging in magnetron sputtering as compared to pulsed laser deposition (PLD) and MOCVD. The PLD technique has been used for over a decade to deposit high quality ZnO films. The principle of this technique is very simple: high power laser pulses are used to remove material from the surface of the target material (ablation), which is then deposited on the substrate. A recent experimental study has been presented by Vinodkumar et al. [37] on structural, optical, and electrical characterization of porous nanostructured ZnO thin films prepared by PLD. The films grown by PLD are free of impurities with good stoichiometric control but inconsistency in thickness and other characteristics of the film is a drawback. It is also a big challenge to deposit uniform films on large area wafers using PLD.

MOCVD, also known as metal organic vapor phase epitaxy (MOVPE), is a well-established technology for the chemical vapor deposition of ZnO thin films. This technique has many advantages; for example, high controllability of the film structure, deposition over large areas, feasibility of commercial scale production, and high temperature growth. Using MOCVD, ZnO layers with improved quality compared to MBE growth can be produced with better reproducibility and growth rate. In 2006, we demonstrated a detailed study of reactor dynamics and kinetics of ZnO growth [38]. The influences of growth temperature, reactor pressure, VI/II ratio, and disk rotation speed on morphological, optical, and electrical properties of ZnO films were investigated. An optimal growth window was determined based on calculations and experimental results. Dry etching of ZnO was also performed to analyze the stability of ZnO in hydrogen at different temperatures. ZnO thin films were grown on c-plane sapphire substrates as well as on GaN buffer layers to evaluate the effects of GaN interlayers on the structural and optical properties of the ZnO epilayers. Diethylzinc (DEZn) and oxygen were used as chemical sources and nitrogen as the carrier gas. The growth temperature was varied from 300 to 600 °C and chamber pressure was varied from 30 to 60 Torr. The disk rotation speed was varied in the range of 600 to 1200 rpm. By changing the oxygen flow rate, VI/II ratio was varied from 220 to 900 with constant DEZn flow rate of 18 μmol/min. Figure 1 shows simulation results for the Reynolds Number (*Re*) of different growth conditions to estimate initial growth windows for disk rotation speed and reactor pressure. Diffusion of adatoms onto the substrate depends on the boundary layer thickness, which decreases with increasing *Re*. The influence of growth temperature on growth rate is illustrated in Figure 2. Growth temperature should have negligible impact on growth rate because sufficient energy is already present in the system since DEZn is completely decomposed at 400 °C. However, growth rate considerably increases with rise in temperature, signifying kinetically oxygen-limited growth. The dependence of carrier concentration

and mobility on VI/II ratio is depicted in Figure 3. The similarity in carrier concentration and RMS surface roughness at higher VI/II ratio suggests that the carrier concentration is mainly due to surface states. Readers should refer to our previously published results for detailed experimental analysis of structural and optical properties of ZnO using high resolution X-ray diffraction (HRXRD), Raman spectroscopy, photoluminescence (PL), optical transmission, ellipsometry, atomic force microscopy (AFM), and scanning electron microscopy [38, 39]. In a recent study we have grown ZnO thin films with different thicknesses on sapphire substrates using MOCVD in our lab [33]. It was demonstrated that crystal quality degrades with an increase in thickness of the ZnO film due to the poor lattice match with the sapphire substrate and growth rate substantially decreases with an increase in growth pressure. Deterioration in crystal quality with increased film thickness is depicted in Figure 4. The film quality can be improved by introducing a thin low temperature buffer layer or MgZnO layer between ZnO and sapphire substrate [10]. We have also reported some experimental results regarding unintentionally doped *n*-type and nitrogen doped *p*-type ZnO films [40-42]. Hall measurements revealed that *n*-type films with carrier concentrations of  $6.57 \times 10^{18} \text{ cm}^{-3}$  and *p*-type films with carrier concentration of  $4.24 \times 10^{14} \text{ cm}^{-3}$  were achieved. Other researchers have also demonstrated *n*-type as well as *p*-type ZnO thin films but it is still a challenge to attain reproducible and highly conductive *p*-type ZnO films and nanostructures.

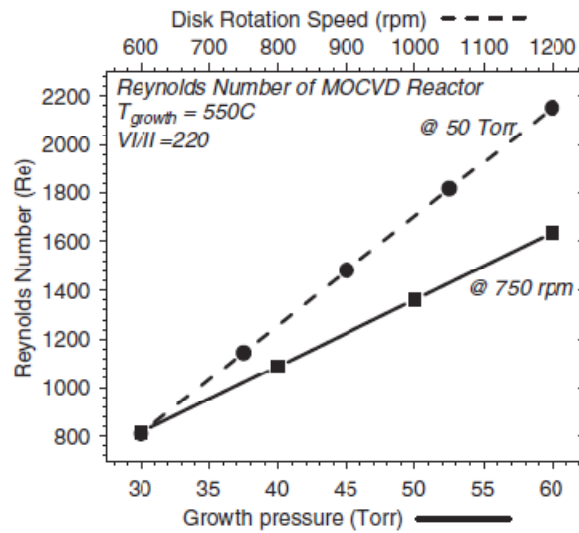


Figure 1. Calculated values of the Reynolds number for different growth conditions. Reynolds number decreases with increasing chamber pressure [38].

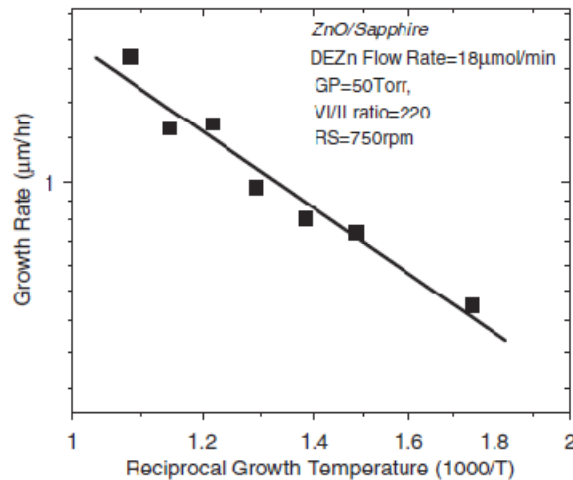


Figure 2. Influence of growth rate on growth temperature. Increase in growth rate with growth temperature suggests kinetically oxygen-limited growth [38].

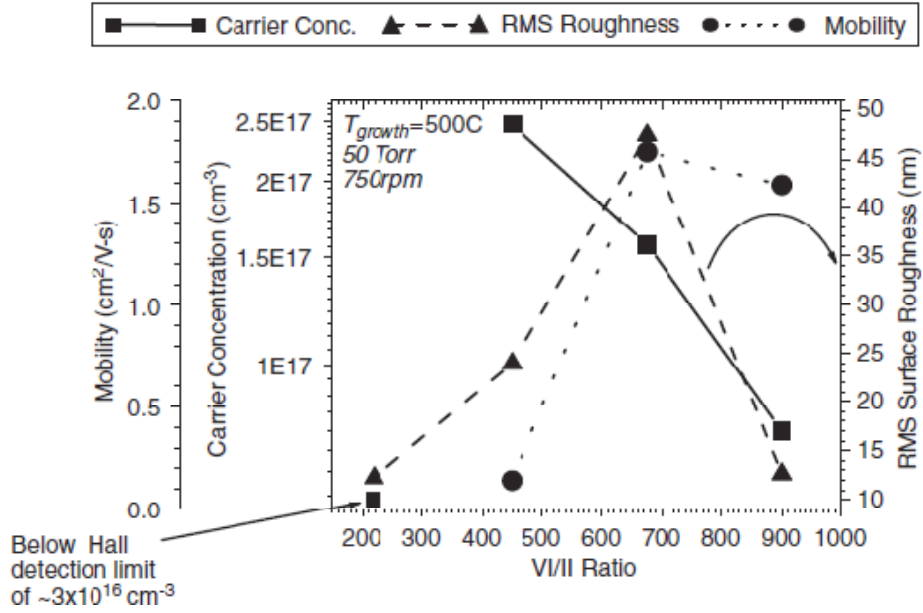


Figure 3. Dependence of electrical properties of ZnO film on VI/II ratio. Same trend in carrier concentration and RMS surface roughness at higher VI/II ratio proves that carrier concentration is mainly due to surface states [38].

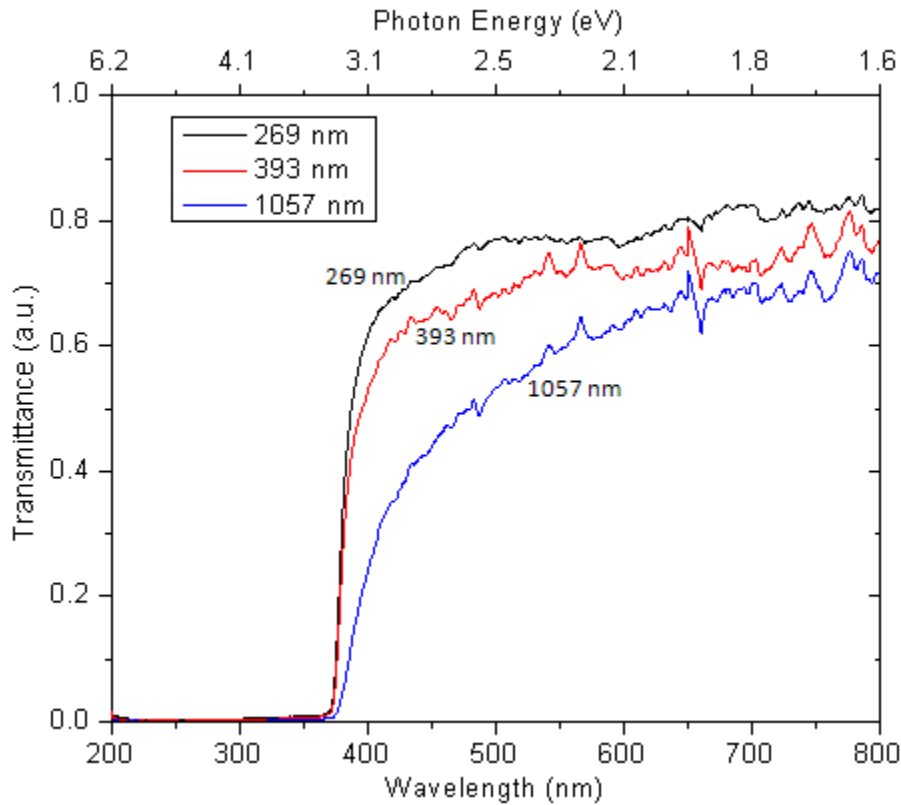


Figure 4. Transmission spectra of ZnO films for three different thicknesses. The annihilation in transmission is mainly because of degradation in crystal quality due to poor lattice match between ZnO and sapphire [33].

### 3. APPLICATIONS

#### 3.1 TFTs and HEMTs

Problems related to p-type doping of ZnO are well known. The FETs may not need pn junctions thereby avoiding p-type doping of ZnO. Therefore, the most feasible and practical application of ZnO is to fabricate unipolar devices, such as high frequency and high power FETs. Major improvements in the electrical and optical properties of field-effect devices due to the formation of a two-dimensional electron gas (2DEG) at the heterostructure interface of ZnO and MgZnO in a strained ZnO potential-well have been reported [43]. In 2008, Tsukazaki et al. achieved high electron mobility ( $14000 \text{ cm}^2\text{V}^{-1}\text{s}^{-1}$ ) at low temperature due to strong two-dimensional confinement of electrons by growing ZnO/MgZnO heterostructures using plasma induced MBE [8]. This work exhibits the possibility of ZnO based high performance HEMTs. Figure 5 shows dependence of mobility and carrier concentration of ZnO/MgZnO heterostructures on temperature as demonstrated by Tsukazaki et al. A similar study demonstrated the mechanism and origin of the two-dimensional electron gas in ZnO/MgZnO heterostructures [9]. The increase in carrier concentration and mobility with incorporation of Magnesium, reported in this study, is illustrated in Fig. 6. The highest carrier concentration and mobility at room temperature were obtained for Magnesium fraction of 0.61.

A scheme for bottom-gated ZnO TFTs with enhanced electrical characteristics grown by MOCVD on a glass substrate was also proposed [10]. The schematic is shown in Fig. 7, which illustrates incorporation of a thin MgZnO layer at the channel-gate insulator interface. The mobility, on/off current ratio, turn on voltage, and sub-threshold slope for ZnO TFTs without MgZnO layer were  $2.3 \text{ cm}^2\text{V}^{-1}\text{s}^{-1}$ ,  $6.4 \times 10^7$ ,  $-6.75 \text{ V}$ , and  $0.78 \text{ V/dec}$  respectively. The same features for ZnO TFTs with MgZnO layer (Fig. 7) were measured as  $9.1 \text{ cm}^2\text{V}^{-1}\text{s}^{-1}$ ,  $2.3 \times 10^8$ ,  $-2.75 \text{ V}$ , and  $0.38 \text{ V/dec}$  respectively. The results achieved in this study are very promising for HEMT-type TFTs based on ZnO/MgZnO heterostructures on a glass substrate. These TFTs can be used in displays, ultraviolet detectors, and transparent electronics.

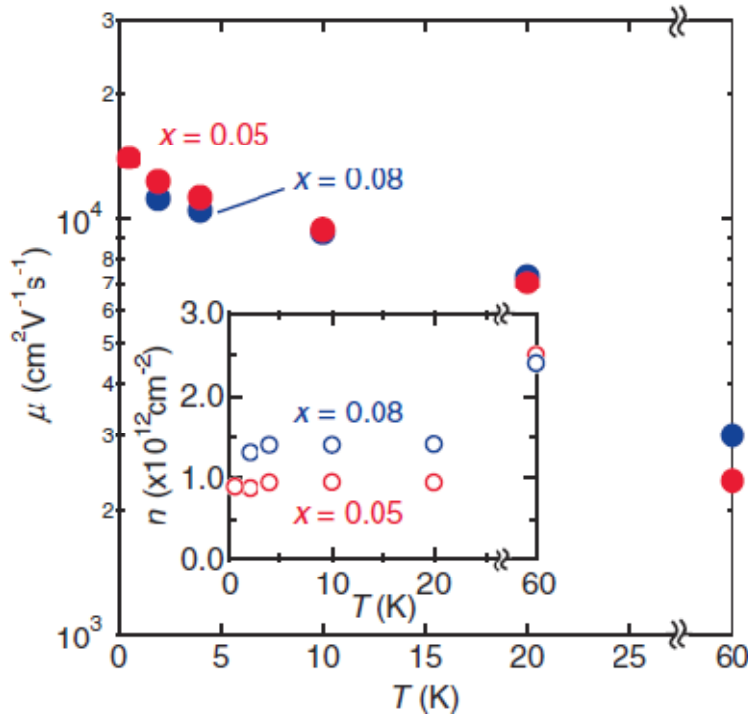


Figure 5. Influence of temperature on electron mobility and electron concentration (inset) of ZnO/MgZnO heterostructures for two different compositions (5% and 8%) of Mg [8].

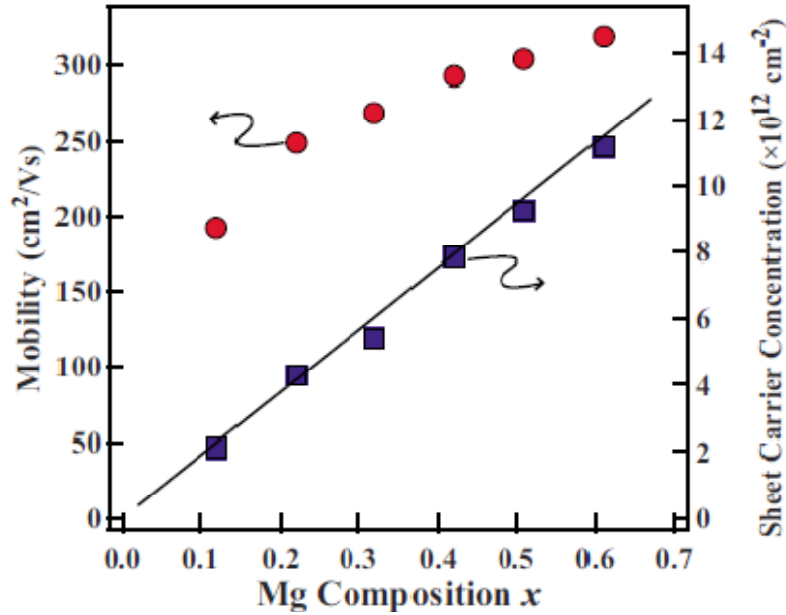


Figure 6. Increase in mobility and carrier concentration with increase in Mg incorporation [9].

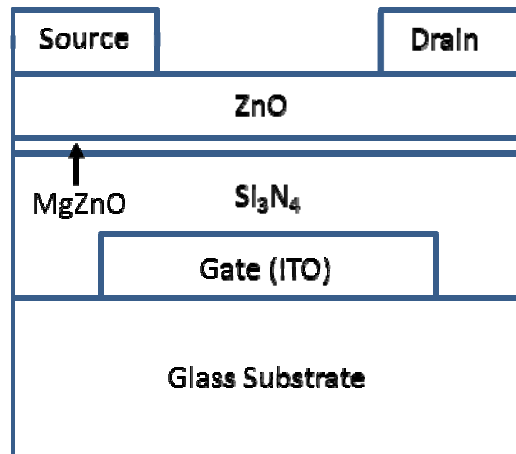


Figure 7. A schematic showing bottom-gate ZnO TFT structure with enhanced electrical characteristics by introducing a thin MgZnO layer at channel-gate insulator interface.

### 3.2 UV Emitters and Detectors

Most of the applications of ZnO such as piezoelectric transducers, phosphors, and TCOs use polycrystalline structure. However, due to recent progress in single crystal bulk growth, ZnO is getting substantial attention for its suitability for fabricating ultraviolet emitters and detectors [44 – 46]. ZnO has a few significant merits over its main competitor material GaN [47]. These advantages include its free exciton energy of 60 meV which is much higher than that of GaN (25 meV), leading to narrowband room-temperature exciton emission and absorption. Native substrates of ZnO are easily available now and wet chemical processing of ZnO is possible. ZnO is more resistant to radiation damage as compared to GaN. In 2005, Nause et al. [48] demonstrated the first electroluminescence (EL) peak measured from ZnO p-n junction LED. The authors prepared an n-type bulk single crystal ZnO using the melt growth technique, and used it as a substrate for homoepitaxial growth of p-type ZnO films to form p-n homojunction structures. Nitrogen was introduced as a p-type dopant into ZnO during MOCVD growth using an NH<sub>3</sub> plasma generated by an RF power supply. Hall measurements on the n-type ZnO yielded carrier concentrations on the order of 10<sup>18</sup> cm<sup>-3</sup> with a mobility of 113 cm<sup>2</sup>/Vs. Excellent optical

transmission from the sharp absorption edge through the visible portion of the spectrum was observed. These measurements suggest that n-type ZnO is a perfect candidate for optical device applications. Post annealing of p-type ZnO films improved I-V characteristics significantly. Figure 8 depicts EL spectrum obtained from devices driven by 40 mA current. A dominant EL peak can be observed at 384 nm which was attributed to recombination from shallow donors to the N luminescent centers on the p side of the junction. In 2010, Namkoong et al. used MBE to prepare heterostructure p-GaN/InGaN/n-ZnO LEDs [49]. A representative PL spectrum and I-V characteristics of the heterojunction device are shown in Figure 9(a) and EL spectra for two different forward currents are presented in Figure 9(b). The authors have attributed the broad yellow band to magnesium related defects in Mg-doped GaN layers.

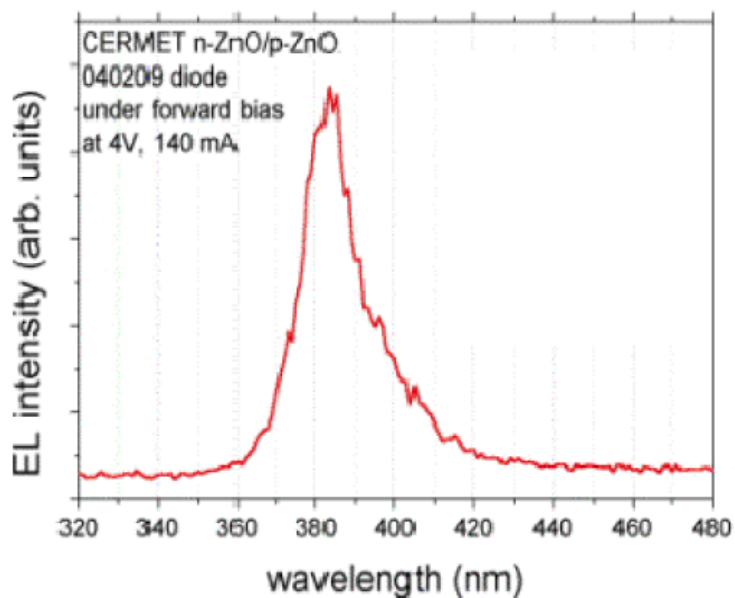


Figure 8. EL spectrum from ZnO p-n junction LED [48].

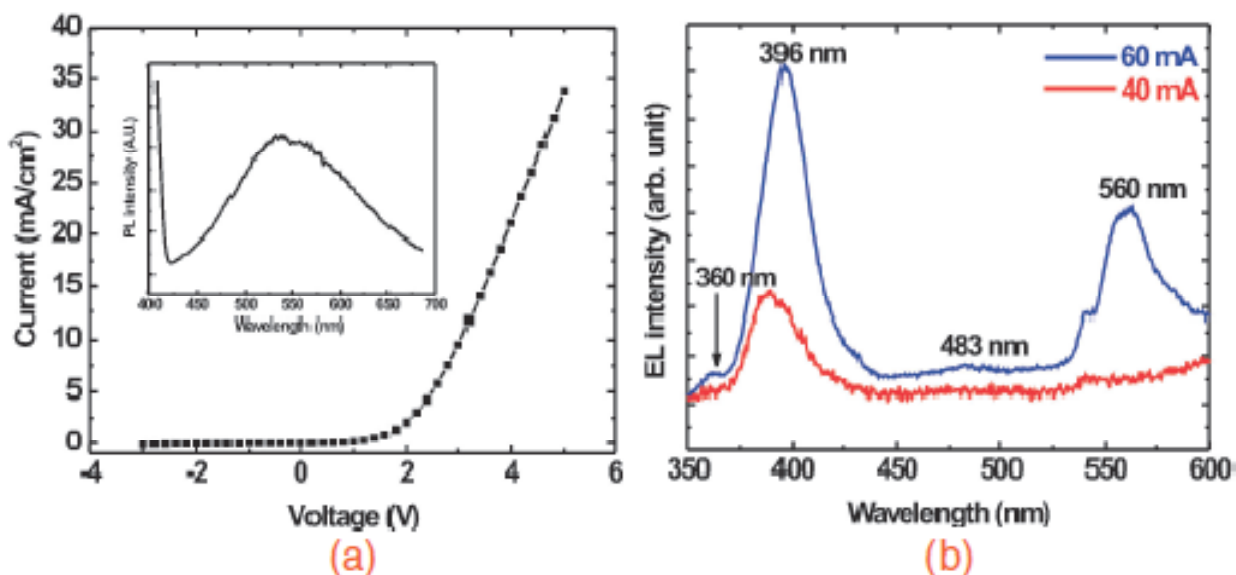


Figure 9. Electrical and optical characterization of heterostructure p-GaN/InGaN/n-ZnO LEDs. (a) I-V characteristics of the heterojunction device. Inset shows PL spectrum measured at room temperature (b) EL spectra of the device for two different forward currents [49].



### 3.3 Neutron Detection

Neutron detection has numerous applications in various fields; for example, instrumentation of nuclear power and research reactors, oil reservoir exploration, investigations in particle physics, morphological characterization of materials, radiation safety, and cosmic ray detection. Since neutrons are not charged particles, their detection is challenging compared to detecting charged particles and ionizing radiation. Scintillation is one of the recognized techniques for neutron detection over large energy range [50]. ZnO has been investigated for decades for scintillation properties due to its ultra-short decay time and near-band-edge emission. In 2007, Edith et al. have demonstrated synthesis and characterization of ZnO:Ga scintillator exhibiting high near-band-edge luminescence and decay time less than 2 ns [51]. In 2011 we reported highly efficient, portable, and economically feasible ZnO based neutron detectors which can replace conventional  $^3\text{He}$  tube technology [52]. A range of ZnO crystals have been grown using the MOCVD technique to investigate the effects of different dopant levels on light transmission, light yield, and decay times. The large exciton binding energy of ZnO results in uniform luminescence of ZnO scintillator up to 500 °C and fast electron-hole recombination during scintillation process. An intrinsic rise time of 30 ps and a decay time of 0.65 ns have been observed which are faster than all other organic or inorganic scintillators available today [52]. Figure 10 illustrates experimental neutron response of undoped ZnO with and without a polyethylene layer. Responses are graphed for  $^{60}\text{Co}$  gamma spectrum and PuBe neutrons spectrum. Calculations revealed that doped ZnO scintillators can have detection efficiencies approaching 100% for thermal neutrons with negligible gamma ray response. The gamma rays response can be minimized by using a thin ZnO epitaxial film. The experimental studies ascertained that ZnO based scintillators for neutron detection can be more efficient with larger surface area and cheaper to fabricate compared to  $^3\text{He}$  tubes.

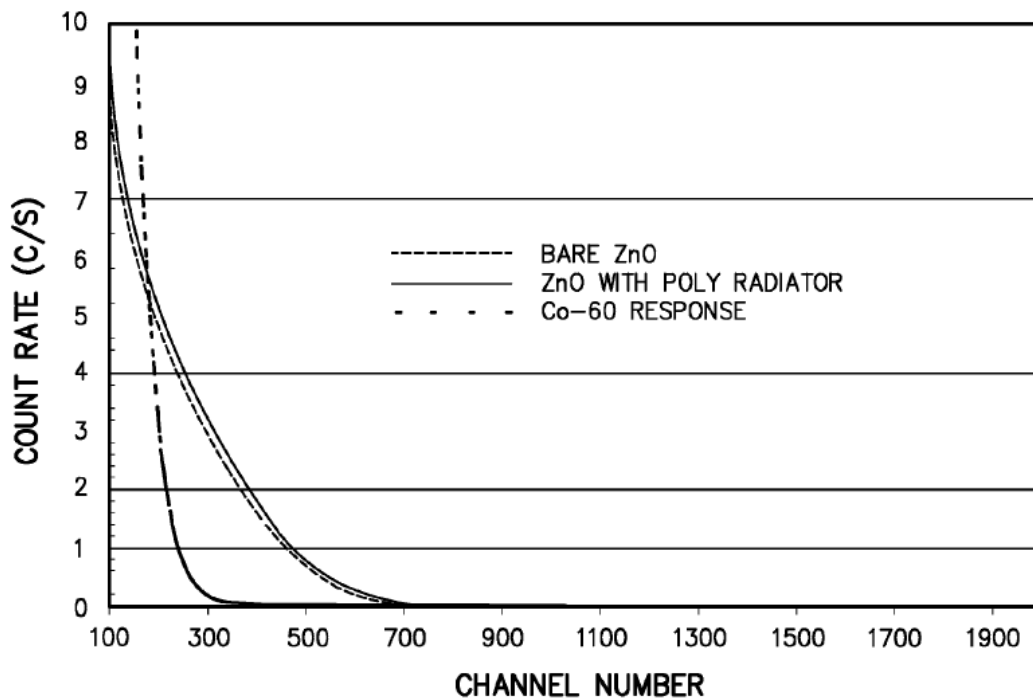


Figure 10. Neutron response of undoped ZnO with and without a polyethylene layer. Responses are given for  $^{60}\text{Co}$  gamma spectrum and PuBe neutrons spectrum [52].

### 3.4 ZnO as Substrate and Interlayer

The wurtzite structure with tetrahedral geometry is the stable form of ZnO with lattice parameters very close to those of GaN, an important wide bandgap semiconductor. This allows fabrication of useful heterostructures of ZnO and GaN for different optical and electronic devices. Also, the  $c/a$  ratio of ZnO wurtzite structure is very close to ideal ratio that supports preparation of stable structures. As mentioned in section 1, our group has presented several studies about use of ZnO as a substrate material for GaN and InGaN [1-4, 17-25]. The mismatch between wurtzite structures of ZnO and GaN is only 1.8% as compared to 13.8 % mismatch between GaN and (0001) Sapphire.

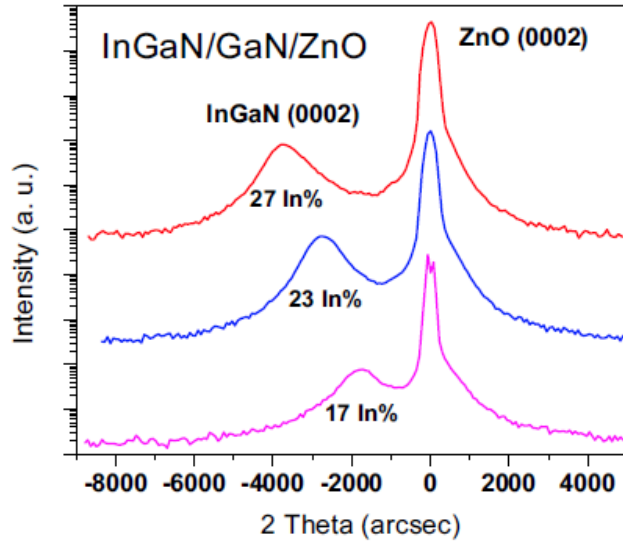


Figure 11. HRXRD  $2\theta/\omega$  scan of InGaN layer with indium compositions of 17%, 23% and 27% grown by MOCVD on ZnO substrates. The samples were grown at 720 °C, 700 °C, and 680 °C respectively [18].

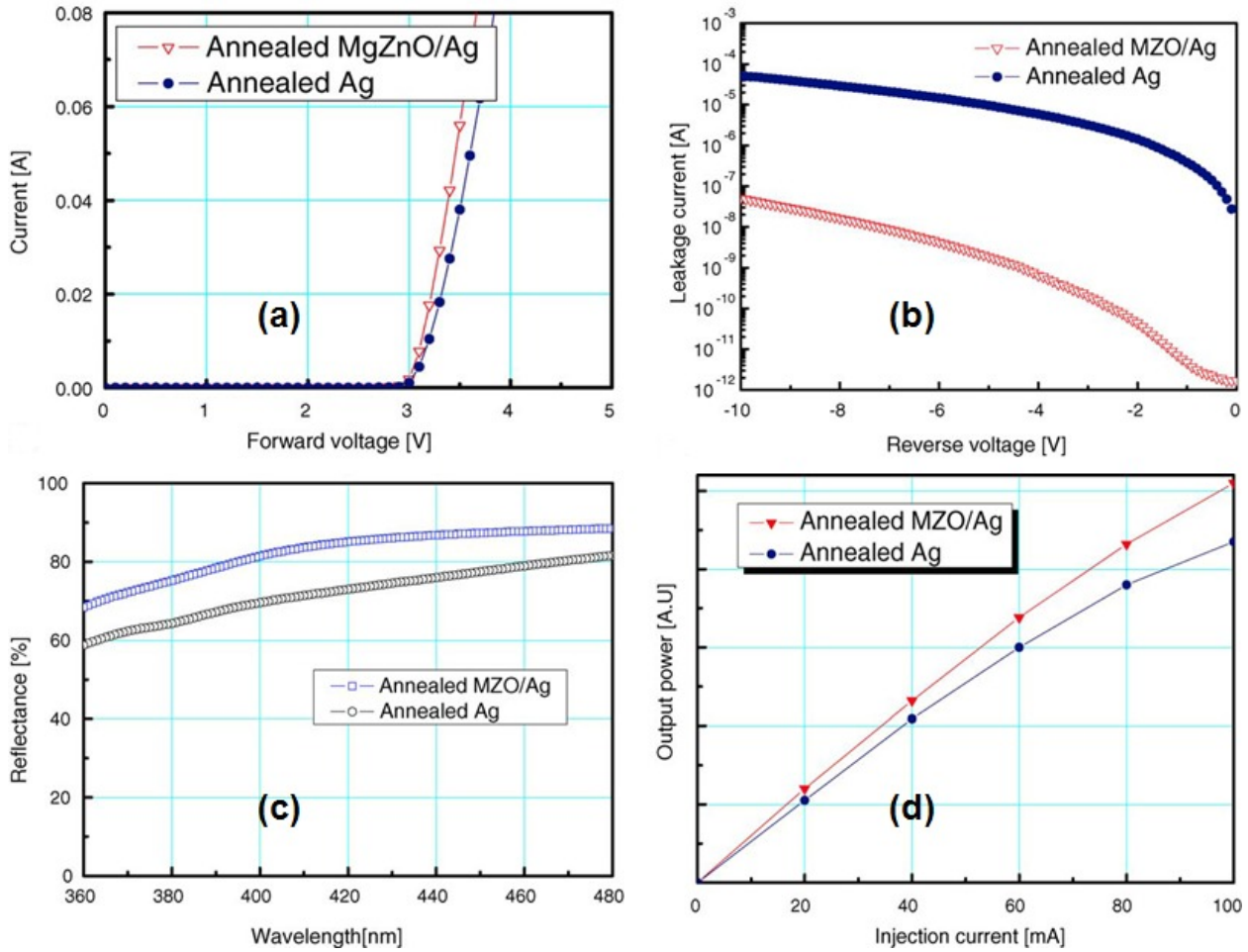


Figure 12. Improvement in the characteristics of annealed MgZnO/Ag contacts as compared with annealed Ag contacts. (a) Forward I-V characteristics (b) reverse I-V characteristics (c) reflectance percentage (d) output power of the LED [54].

InGaN has a perfect lattice match with ZnO in a-axis direction with 18% indium composition [20]. The thermal expansion coefficient of ZnO and GaN is similar resulting in almost zero thermal strain. Furthermore, ZnO substrates are conductive allowing for multiple electrodes on both surfaces for increased current spreading and improved electrical quality of the device. Therefore, ZnO is a perfect substrate for GaN and InGaN devices as compared to sapphire and SiC. Figure 11 shows HRXRD scan of InGaN layer with three different indium compositions grown by MOCVD on ZnO substrates [18]. We have also successfully grown AlGaIn/GaN superlattice structures on ZnO substrates using MOCVD for green emitter applications [53]. The improvement in structural and optical properties of the superlattices was verified by XRD, AFM, and PL measurements.

Silver (Ag), due to its high reflectivity and good Ohmic behavior, is the most commonly used back contact for flip-chip LEDs. But Ag electrodes experience problems of agglomeration and interfacial voids upon annealing, which in turn degrade electrical and optical performance of the device. It was demonstrated that LEDs fabricated with MgZnO interlayer between GaN and Ag contact exhibited better performance as compared with the LEDs without interlayer [54]. Figure 12 shows difference between the characteristics of annealed MgZnO/Ag contacts and annealed Ag contacts.

### 3.5 Thermoelectric Power Generation

Thermoelectric (TE) effect is the transformation of temperature difference to electromotive force (Seebeck effect) and vice versa (Peltier effect). Generation of electricity using TE effect is one of the promising methods to obtain usable energy directly from waste heat and natural heat resources consequently improving the efficiency of energy use and reducing the consumption of main sources of CO<sub>2</sub> emission. It is anticipated that TE power generation can greatly contribute to overcoming the unequivocal problems of global warming and climate change [55]. Thermoelectric materials are characterized on the basis of a dimensionless figure of merit that depends on temperature ' $T$ ' and expressed as  $ZT = S^2\sigma T\kappa^{-1}$  where  $S$ ,  $\sigma$ , and  $\kappa$  are Seebeck coefficient, electrical conductivity and thermal conductivity respectively, the parameters associated with the material. The semiconductors used for thermoelectric cooling like Bi<sub>2</sub>Te<sub>3</sub>, PbTe and related materials are toxic, expensive, heavy and can melt or oxidize at high temperatures, therefore, cannot be employed for widespread heat harvesting in air atmosphere. Oxide materials are most promising candidates in these conditions. Compared to p-type oxides, n-type oxides have not been developed yet despite continuous efforts [55]. In such an attempt, Yamaguchi et al. have investigated thermoelectric properties of Al-doped ZnO co-doped with transition metals Fe, Ni, and Sm [56]. Experimental results of the TE parameters are illustrated in Figure 13. The Seebeck coefficient was improved by Sm co-doping and electrical conductivity was enhanced by Ni co-doping. The  $\kappa$  value at 1073 K for Ni-co-doped ZnO:Al was 77% of that for ZnO:Al. The ZT value of 0.126 was achieved at 1073 K for Ni-co-doped ZnO:Al representing an improvement by a factor of 1.5 as compared to ZnO:Al. Nevertheless, electron mobility was deteriorated with co-doping transition metals. Similarly, Tsubota et al. have reported maximum ZT value of 0.3 achieved at 1000 °C [57]. In our Lab, we have studied TE characteristics of ZnO:Al for different doping concentrations at room temperature. The impact of carrier concentration on mobility ( $\mu$ ), electrical conductivity, Seebeck coefficient, and power factor ( $S^2\sigma$ ) is shown in Figure 14(a) and 14(b). It can be noticed that Seebeck coefficient linearly decreases with increasing carrier concentration which is commonly observed TE behavior. The highest Seebeck coefficient of 827  $\mu$ V/K was measured at carrier concentration of  $1.38 \times 10^{16}$  cm<sup>-3</sup>. The power factor increases with carrier concentration except one point  $1 \times 10^{17}$  cm<sup>-3</sup>. This can be attributed to major trade-off between Seebeck coefficient and mobility which is lowest at the same carrier concentration (Figure 14(a)). The highest value of power factor was found to be  $0.748 \times 10^{-4}$  Wm<sup>-1</sup>K<sup>-2</sup> at carrier concentration of  $2.04 \times 10^{17}$  cm<sup>-3</sup>. The results presented by Yamaguchi et al., Tsubota et al. and our group are encouraging but still extensive efforts are required to make ZnO feasible for TE power generation.

One effective way to achieve high ZT is by engineering nanostructured materials. The mean free path of phonon (responsible for thermal conduction) is larger by few orders than mean free path of electrons (associated with electric conduction). Nanostructures of different sizes can be incorporated in the material to enhance boundary scattering of short-, medium-, and long-wavelength acoustic phonons causing reduced  $\kappa$  without affecting electron transport. Nanostructures have been successfully employed to reduce  $\kappa$  resulting in improved ZT value [58, 59]. Due to unique physical properties and highly stable wurtzite crystal structure, ZnO is a material whose nanostructural configurations are much richer than any known nanomaterial including carbon nanotubes [60]. Using vapor transport process while controlling the growth kinetics, temperature, and chemical composition of precursors, a variety of nanostructures can be synthesized [61]. Therefore, ZnO nanostructures can be considered as potential candidate for TE devices.

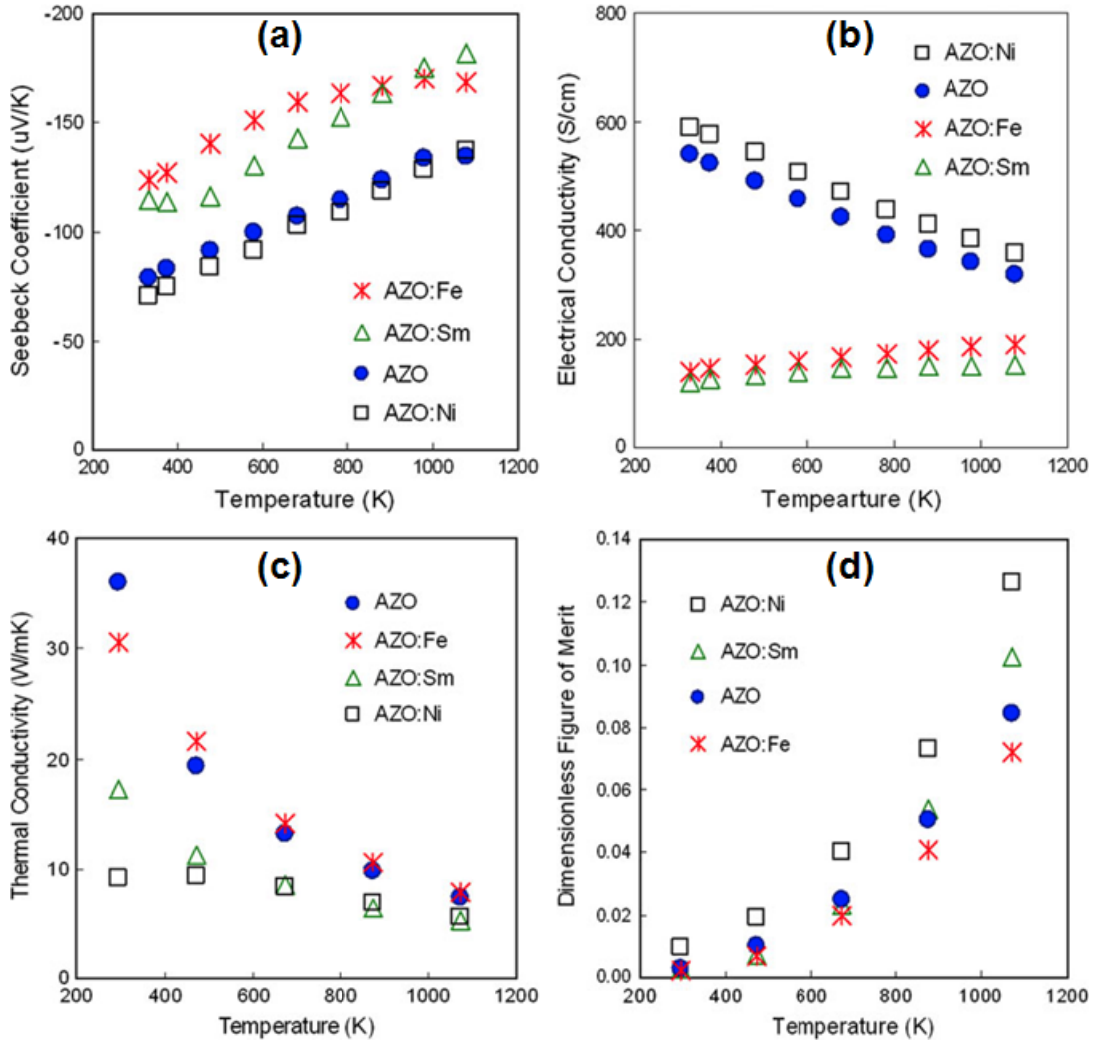


Figure 13. Influence of temperature on thermoelectric parameters of ZnO:Al co-doped with different transition metals. (a) Seebeck coefficient  $S$  (b) Electrical conductivity  $\sigma$  (c) Thermal conductivity  $\kappa$  (d) Figure of merit  $ZT$  [56].

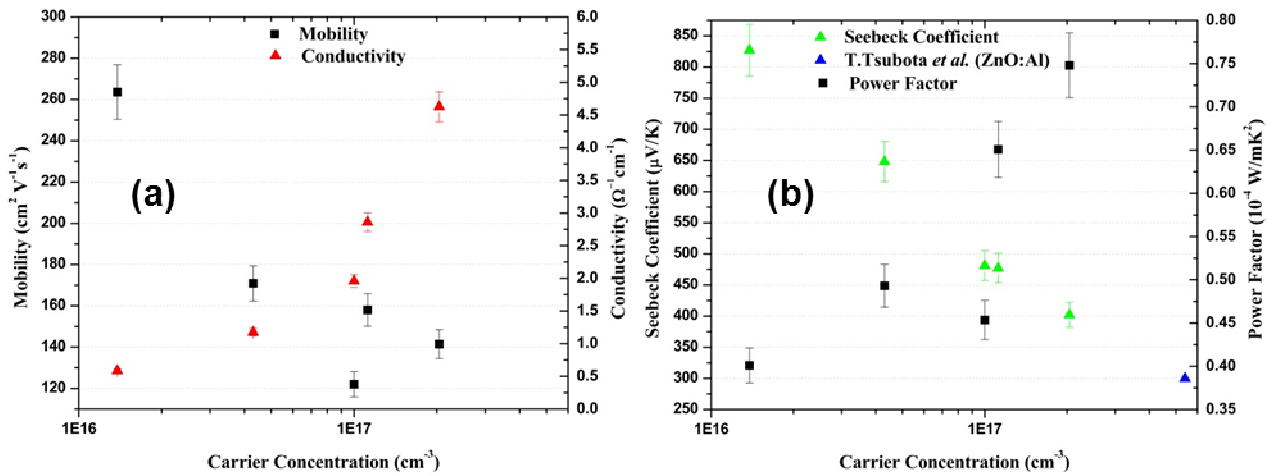


Figure 14. The impact of carrier concentration on (a) mobility, electrical conductivity, (b) Seebeck coefficient, and power factor.

## 4. CONCLUSION

We have presented a brief review on synthesis and applications of ZnO. After highlighting unique characteristics of ZnO, we have discussed commonly used techniques for its growth including MBE, magnetron sputtering, and PLD. The most reliable and feasible technique for ZnO growth, MOCVD, was emphasized. Previous experimental results regarding growth and characterization of ZnO using MOCVD in our lab as well as results reported by other groups were presented in detail. Modern applications under investigation including TFTs and HEMTs, UV emitters and detectors, and thermoelectric power generation were explained and related experimental results were presented. The use of ZnO in neutron detection, a novel application, previously reported by our group was illustrated with experimental evidence. Moreover, suitability of ZnO as substrate or interlayer material was also discussed summarizing our previously reported results. The review shows that ZnO is undoubtedly a quickly evolving material in semiconductor field. However, concentrated efforts are required to understand the principles behind growth of doped and undoped ZnO films and nanostructures to make it acceptable for the semiconductor industry.

## REFERENCES

- [1] Huang, I. H., Lan, Y. R., Wu, T. H., Feng, Z. C., Li, N., Yu, H., Ferguson, I., and Lu, W., "Nanoscale InGaN/GaN on ZnO substrate for LED applications," Proc. SPIE 7422, 74220K-1-12 (2009).
- [2] Melton, A., Jampana, B., Li, N., Jamil, M., Zaidi, T., Fenwick, W., Opila, R., Honsberg, C., and Ferguson, I., "High indium composition (>20%) InGaN epi-layers on ZnO substrates for very high efficiency solar cells," Proc. IEEE 978, 001123-001126 (2009).
- [3] Li, N., Wang, S. J., Huang, C. L., Feng, Z. C., Valencia, A., Nause, J., Summers, C., and Ferguson, I., "Effect of an Al<sub>2</sub>O<sub>3</sub> transition layer on InGaN on ZnO substrates by organometallic vapor-phase epitaxy," J. Crystal Growth 310(23), 4908-4912 (2008).
- [4] Wang, S. J., Li, N., Yu, H. B., Feng, Z. C., Summers, C., and Ferguson, I., "Metalorganic chemical vapour deposition of GaN layers on ZnO substrates using  $\alpha$ -Al<sub>2</sub>O<sub>3</sub> as a transition layer," J. Phys. D: Appl. Phys. 42(24), 245302-1-5 (2009).
- [5] Wang, Z. L., "Zinc oxide nanostructures: growth, properties and applications," J. Phys.: Condens. Matter. 16(25) R829-R858 (2004).
- [6] Fortunato, E. M. C., Pereira, L. M. N., Barquinha, P. M. C., Rego, A. M. B. D., Goncalves, G., Vila, A., Morante, J. R., and Martins, R. F. P., "High mobility indium free amorphous oxide thin film transistors," Appl. Phys. Lett. 92(22), 222103-1-4 (2008).
- [7] Fortunato, E., Barquinha, P., and Martins, R., "Oxide semiconductor thin-film transistors: a review of recent advances," Adv. Mater. 24(22), 2945-2986 (2012).
- [8] Tsukazaki, A., Yuji, H., Akasaka, S., Tamura, K., Nakahara, K., Tanabe, T., Takasu, H., Ohtomo, A., and Kawasaki, M., "High electron mobility exceeding 104 cm<sup>2</sup>V<sup>-1</sup>s<sup>-1</sup> in Mg<sub>x</sub>Zn<sub>1-x</sub>O/ZnO single heterostructures grown by molecular beam epitaxy," Appl. Phys. Express 1(5), 055004-1-3 (2008).
- [9] Tampo, H., Shibata, H., Maejima, K., Yamada, A., Matsubara, K., Fons, P., Kashiwaya, S., Niki, S., Chiba, Y., Wakamatsu, T., and Kanie, H., "Polarization-induced two-dimensional electron gases in ZnMgO/ZnO heterostructures," Appl. Phys. Lett. 93(20), 202104-1-3 (2008).
- [10] Remashan, K., Choi, Y. S., Park, S. J., and Jang, J. H., "High performance MOCVD-grown ZnO thin-film transistor with a thin MgZnO layer at channel/gate insulator interface," J. Electrochem. Soc. 157(12), H1121-H1126 (2010).
- [11] Nayak, P. K., Yang, J., Kim, J., Chung, S., Jeong, J., Lee, C., and Hong, Y., "Spin-coated Ga-doped ZnO transparent conducting thin films for organic light-emitting diodes," J. Phys. D: Appl. Phys. 42(3), 035102-1-6 (2009).
- [12] Huang, Y. C., Li, Z. Y., Chen, H. H., Uen, W. Y., Lan, S. M., Liao, S. M., Huang, Y. H., Ku, C. T., Chen, M. C., Yang, T. N., and Chiang, C. C., "Characterizations of gallium-doped ZnO films on glass substrate prepared by atmospheric pressure metal-organic chemical vapor deposition," Thin Solid Films 517(18), 5537-5542 (2009).
- [13] Zhao, J., Sun, X. W., and Tan, S. T., "Bandgap-engineered Ga-rich GaZnO thin films for UV transparent electronics," Proc. IEEE 56(12), 2995-2999 (2009).
- [14] Ye, J. D., Gu, S. L., Zhu, S. M., Liu, S. M., Zheng, Y. D., Zhang, R., Shi, Y., Yu, H. Q., and Ye, Y. D., "Gallium doping dependence of single-crystal n-type ZnO grown by metal organic chemical vapor deposition," J. Crystal Growth 283(3-4), 279-285 (2005).

- [15] Hahn, B., Heindel, G., Schoberer, E. P., and Gebhardt, W., "MOCVD layer growth of ZnO using DMZn and tertiary butanol," *Semicond. Sci. Technol.*, 13(7), 788-791 (1998).
- [16] Hirata, G. A., McKittrick, J., Cheeks, T., Siqueiros, J. M., Diaz, J. A., Contreras, O., and Lopez, O. A., "Synthesis and optoelectronic characterization of gallium doped zinc oxide transparent electrodes," *Thin Solid Films* 288(1-2), 29-31 (1996).
- [17] Li, N., Park, E. H., Huang, Y., Wang, S., Valencia, A., Nemeth, B., Nause, J., and Ferguson, I., "Growth of GaN on ZnO for solid state lighting applications," *Proc. SPIE* 6337, 63370Z-1-6 (2006).
- [18] Wang, S. J., Li, N., Park, E. H., Feng, Z. C., Valencia, A., Nause, J., Kane, M., Summers, C., and Ferguson, I., "MOCVD growth of GaN-based materials on ZnO substrates," *Phys. Stat. Sol. (c)* 5(6), 1736-1739 (2008).
- [19] Li, N., Wang, S. J., Park, E. H., Feng, Z. C., Tsai, H. L., Yang, J. R., and Ferguson, I., "Suppression of phase separation in InGaN layers grown on lattice-matched ZnO substrates," *J. Crystal Growth* 311(22), 4628-4631 (2009).
- [20] Wang, S. J., Li, N., Park, E. H., Lien, S. C., Feng, Z. C., Valencia, A., Nause, J., and Ferguson, I., "Metalorganic chemical vapor deposition of InGaN layers on ZnO substrates," *J. Appl. Phys.* 102(10), 106105-1-3 (2007).
- [21] Li, N., Wang, S. J., Park, E. H., Feng, Z. C., Valencia, A., Nause, J., Summers, C., and Ferguson, I., "Growth of InGaN with high indium content on ZnO based sacrificial substrates," *Proc. SPIE* 6669, 66690X-1-7 (2007).
- [22] Li, N., Wang, S. J., Huang, C. L., Feng, Z. C., Valencia, A., Nause, J., Summers, C., and Ferguson, I., "Metalorganic chemical vapor deposition of GaN and InGaN on ZnO substrate using Al<sub>2</sub>O<sub>3</sub> as a transition layer," *Proc. SPIE* 7058, 70580K-1-6 (2008).
- [23] Li, N., Wang, S. J., Park, E. H., Feng, Z. C., Tsai, H. L., Yang, J. R., Valencia, A., Nause, J., Summers, C., and Ferguson, I., "Influence of high indium composition InGaN on lattice matched ZnO sacrificial substrates," *J. Light & Vis. Env.* 32(2), 143-147 (2008).
- [24] Fenwick, W. E., Li, N., Jamil, M., Xu, T., Melton, A., Wang, S., Yu, H., Valencia, A., Nause, J., Summers, C., and Ferguson, I. T., "Development of new substrate technologies for GaN LEDs: atomic layer deposition transition layers on silicon and ZnO," *Proc. SPIE* 7231, 723119-1-9 (2009).
- [25] Li, N., Fenwick, W., Melton, A., Hung, I. H., Feng, Z. C., Summers, C., Jamil, M., and Ferguson, I., "III-nitride epilayers on ZnO substrates by MOCVD using Al<sub>2</sub>O<sub>3</sub> as a transition layer," *Proc. SPIE* 7422, 74220J-1-8 (2009).
- [26] Kane, M. H., Shalini, K., Summers, C. J., Varatharajan, R., Nause, J., Vestal, C. R., Zhang, Z. J., and Ferguson, I. T., "Magnetic properties of bulk Zn<sub>1-x</sub>Mn<sub>x</sub>O and Zn<sub>1-x</sub>Co<sub>x</sub>O single crystals," *J. Appl. Phys.* 97(2), 023906-1-6 (2005).
- [27] Kane, M. H., Fenwick, W. E., Strassburg, M., Nemeth, B., Varatharajan, R., Song, Q., Keeble, D. J., Mkami, H. E., Smith, G. M., Zhang, Z. J., Nause, J., Summers, C. J., and Ferguson, I. T., "Magnetic and optical properties of single crystals of transition metal doped ZnO," *Phys. Stat. Sol. (b)* 244(5), 1462-1467 (2007).
- [28] Fenwick, W. E., Kane, M. H., Varatharajan, R., Zaidi, T., Fang, Z., Nemeth, B., Keeble, D. J., Mkami, H. E., Smith, G. M., Nause, J., Summers, C. J., and Ferguson, I. T., "Transition metal- and rare earth-doped ZnO: a comparison of optical, magnetic, and structural behavior of bulk and thin films," *Proc. SPIE* 6474, 64741Q-1-8 (2007).
- [29] Gupta, S., Fenwick, W. E., Melton, A., Zaidi, T., Yu, H., Rengarajan, V., Nause, J., Ougazzaden, A., and Ferguson, I. T., "MOVPE growth of transition-metal-doped GaN and ZnO for spintronic applications," *J. Crystal Growth* 310(23), 5032-5038 (2008).
- [30] Lo, K. Y., Huang, Y. J., Huang, J. Y., Feng, Z. C., Fenwick, W. E., Pan, M., and Ferguson, I. T., "Reflective second harmonic generation from ZnO thin films: a study on the Zn-O bonding," *Appl. Phys. Lett.* 90(16), 161904-1-3 (2007).
- [31] Ganesan, S., Feng, Z. C., Mehta, D., Kandoor, S., Wornyo, E. J., Nause, J., and Ferguson, I., "Optical properties of bulk and epitaxial ZnO for waveguide applications," *Proc. MRS* 799(1), (2003).
- [32] Burgett, E. A., Hurwitz, E. N., Hertel, N. E., Summers, C. J., Nause, J., Lu, N., and Ferguson, I. T., "Growth of ZnO for neutron detectors," Chapter 12, *Handbook of zinc oxide and related materials (by Z. C. Feng): Volume 2 – Devices and Nano-Engineering*, Published by CRC Press Taylor and Francis Group, 435-483 (2012).
- [33] Hussain, B., Raja, M. Y. A., Lu, N., and Ferguson, I., "Applications and synthesis of zinc oxide: an emerging wide bandgap material," *Proc. IEEE*, in Press.
- [34] Asghar, M., Mahmood, K., Ferguson, I. T., Raja, M. Y. A., Xie, Y. H., Tsu, R., and Hasan, M. A., "Investigation of V<sub>O</sub>-Zn<sub>i</sub> native donor complex in MBE grown bulk ZnO," *Semicond. Sci. Technol.* 28(10), 105019-1-5 (2013).
- [35] Assuncao, V., Fortunato, E., Marques, A., Aguas, H., Ferreira, I., Costa, M. E. V., and Martins, R., "Influence of the deposition pressure on the properties of transparent and conductive ZnO:Ga thin-film produced by r.f. sputtering at room temperature," *Thin Solid Films* 427(1-2), 401-405 (2003).

- [36] Yu, X., Ma, J., Ji, F., Wang, Y., Zhang, X., Cheng, C., and Ma, H., "Preparation and properties of ZnO:Ga films prepared by r.f. magnetron sputtering at low temperature," *Appl. Surf. Sci.* 239(2), 222-226 (2005).
- [37] Vinodkumar, R., Navas, I., Porsezian, K., Ganesan, V., Unnikrishnan, N. V., and Pillai, V. P. M., "Structural, spectroscopic and electrical studies of nanostructured porous ZnO thin films prepared by pulsed laser deposition," *Spectrochim. Acta Mol. Biomol. Spectros.* 118, 724-732 (2013).
- [38] Pan, M., Fenwick, W. E., Strassburg, M., Li, N., Kang, H., Kane, M. H., Asghar, A., Gupta, S., Varatharajan, R., Nause, J., Zein, N. E., Fabiano, P., Steiner, T., and Ferguson, I., "Metal-organic chemical vapor deposition of ZnO," *J. Crystal Growth* 287(2), 688-693 (2006).
- [39] Chung, Y. L., Li, L., Yao, S., Feng, Z. C., Fenwick, W. E., Zaidi, T., Ferguson, I. T., and Lu, W., "Rutherford backscattering and optical studies for ZnO thin films on sapphire substrates grown by metalorganic chemical vapor deposition," *Proc. SPIE* 7784, 778416-1-10 (2010).
- [40] Zaidi, T., Melton, A., and Fenwick, W. E., "*n*-type, *p*-type and semi-insulating ZnO:N thin film growth by metal organic chemical vapor deposition with NH<sub>3</sub> doping," *J. Vac. Sci. Technol. B* 27(4), 1904-1908 (2009).
- [41] Zaidi, T., Fenwick, W. E., Melton, A., Li, N., Gupta, S., Yu, H., Ougazzaden, A., and Ferguson, I., "Effects of N doping on ZnO thin films grown by MOVPE," *J. Crystal Growth* 310(23), 5011-5015 (2008).
- [42] Pan, M., Nause, J., Rengarajan, V., Rondon, R., Park, E. H., and Ferguson, I. T., "Epitaxial growth and characterization of *p*-type ZnO," *J. Electron. Mater.* 36(4), 457-461 (2007).
- [43] Koike, K., Hama, K., Takada, G. Y., Ozaki, M., Ogata, K. I., Sasa, S., Inoue, M., and Yano, M., "Piezoelectric carrier confinement by lattice mismatch at ZnO/Zn<sub>0.6</sub>Mg<sub>0.4</sub>O heterointerface," *Jpn. J. Appl. Phys.* 43(10B), L 1372-L 1375 (2004).
- [44] Pearton, S. J., Norton, D. P., Ip, K., Heo, Y. W., and Steiner, T., "Recent progress in processing and properties of ZnO," *Prog. Mater. Sci.* 50(3), 293-340 (2005).
- [45] Pearton, S. J., Heo, W. H., Ivill, M., Norton, D. P., and Steiner, T., "Dilute magnetic semiconducting oxides," *Semicond. Sci. Technol.* 19(10), R59-R74 (2004).
- [46] Look, D. C., and Claflin, B., "P-type doping and devices based on ZnO," *Phys. Stat. Sol. (b)* 241(3), 624-630 (2004).
- [47] Look, D. C., "Recent advances in ZnO materials and devices," *Mat. Sci. Eng. B* 80(1-3), 383-387 (2001).
- [48] Nause, J., Pan, M., Rengarajan, V., Nemeth, W., Ganesan, S., Payne, A., Li, N., and Ferguson, I., "ZnO semiconductors for lighting," *Proc. SPIE* 5941, 59410D-1-8 (2005).
- [49] Namkoong, G., Trybus, E., Cheung, M. C., Doolittle, W. A., Cartwright, A. N., Ferguson, I., Seong, T. Y., and Nause, J., "Dual-color emission in hybrid III-nitride/ZnO light emitting diodes," *Appl. Phys. Exp.* 3(2), 022101-1-3 (2010).
- [50] Miresghhi, A., Cho, G., Drewery, J. S., Hong, W. S., Jing, T., Lee, H., Kaplan, S. N., and Mendez, V. P., "High efficiency neutron sensitive amorphous silicon pixel detectors," *Proc. IEEE* 41(4), 915-921 (1994).
- [51] Courchesne, E. D. B., Derenzo, S. E., and Weber, M. J., "Semiconductor scintillators ZnO and PbI<sub>2</sub>: co-doping studies," *Nuclear Instruments and Methods in Physics Research A* 579(1), 1-5 (2007).
- [52] Burgett, E. A., Hertel, N. E., Nause, J. E., and Ferguson, I., "Thin film doped ZnO neutron detectors," US Patent, US 2011/0266448 A1 (2011).
- [53] Yu, H., Wang, S., Li, N., Fenwick, W., Melton, A., Klein, B., and Ferguson, I., "MOVPE growth of AlGaIn/GaN superlattices on ZnO substrates for green emitter applications," *J. Crystal Growth* 310(23), 4904-4907 (2008).
- [54] Hong, H. G., Song, J. O., Lee, T., Ferguson, I. T., Kwak, J. S., and Seong, T. Y., "Improvement of the reverse leakage behavior of Ag-based ohmic contacts for GaN-based light-emitting diodes using MgZnO interlayer," *Material Science and Engineering B* 129(1-3), 176-179 (2006).
- [55] Koumoto, K., Wang, Y., Zhang, R., Kosuga, A., and Funahashi, R., "Oxide thermoelectric materials: a nanostructuring approach," *Annu. Rev. Mater. Res.* 40, 363-394 (2010).
- [56] Yamaguchi, H., Chonan, Y., Oda, M., Komiyama, T., Aoyama, T., and Sugiyama, S., "Thermoelectric properties of ZnO ceramics co-doped with Al and transition metals," *J. Electron. Mater.* 40(5), 723-727 (2011).
- [57] Tsubota, T., Ohtaki, M., Eguchi, K., and Arai, H., "Thermoelectric properties of Al-doped ZnO as a promising oxide material for high temperature thermoelectric conversion," *J. Mater. Chem.* 7(1), 85-90 (1997).
- [58] Majumdar, A., "Thermoelectricity in semiconductor nanostructures," *Science* 303(5659), 777-778 (2004).
- [59] Li, D., Wu, Y., Fan, R., Yang, P., and Majumdar, A., "Thermal conductivity of Si/SiGe superlattice nanowires," *Appl. Phys. Lett.* 83(15), 3186-3188 (2003).
- [60] Wang, Z. L., "Nanostructures of zinc oxide," *Mater. Today* 7(6), 26-33 (2004).
- [61] Fan, Z., and Lu, J. G., "Zinc oxide nanostructures: synthesis and properties," *J. Nanosci. Nanotechnol.* 5(10), 1561-1573 (2005).